J. Membrane Biol. 188, 43–53 (2002)
DOI: 10.1007/s00232-001-0172-4

The Journal of
Membrane
Biology

Molecular and Cellular Characterization of a Water-Channel Protein, AQP-h3, Specifically Expressed in the Frog Ventral Skin

H. Tanii*, T. Hasegawa*, N. Hirakawa, M. Suzuki, S. Tanaka
Department of Biology, Faculty of Science, Shizuoka University, Ohya 836, Shizuoka 422-8529, Japan

Received: 9 November 2001/Revised: 8 March 2002

Abstract. Two cDNAs encoding frog aquaporin (AQP) were cloned from a cDNA library constructed for the ventral skin of the tree frog, *Hyla japonica* and sequenced. One AQP (*Hyla* AQP-h1) consisted of 271 amino-acid residues with high homology to toad AQP-t1, *Rana* CHIP28 (AQP1), and rat AQP1. The other AQP (AQP-h3) consisted of 271 amino-acid residues with higher homology to mammalian AQP2 than to mammalian AQP3. The predicted amino-acid sequence contained the conserved two NPA motifs found in all MIP family members and the putative six transmembrane domains. The sequence also confers mercurial sensitivity, which is common to all the AQPs except AQP0, AQP4 and AQP7. Potential N-glycosylation sites were present at Asn-44 in AQP-h1, and at Asn-124 and Asn-125 in AQP-h3. In addition, AQP-h3 had a putative phosphorylation site by protein kinase A at Ser-255, which is identical to mammalian AQP2. In swelling assays using *Xenopus* oocytes, AQP-h1 facilitates water permeability, whereas AQP-h3 displayed weak water permeability. Searching for the expression of these two AQP mRNAs revealed that AQP-h1 was expressed in most tissues, whereas AQP-h3 was observed only in the ventral skin. An antibody (ST-141) against the C-terminal peptide of the AQP-h3 protein recognized a 29.0 kDa-protein with a molecular mass close to that of the *Hyla* AQP-h3 protein and immunostained predominantly in the abdominal pelvic skin. In pelvic skin, the label for AQP-h3 was more intense in the upper layer of the stratum granulosum and was localized to both the apical and basolateral plasma membranes of the principal cells. These findings suggest that *Hyla* AQP-h3 plays a pivotal role in constitutively absorbing water from ventral pelvic skin.

Correspondence to: S. Tanaka; email: sbstana@ipc.shizuoka.ac.jp
* H.T. and T.H. contributed equally to this work

Key words: Water channel — Aquaporin — cDNA — mRNA expression — Anti-peptide antibody — Immunohistochemistry — Skin — Frog

Introduction

Water movement occurs across plasma membranes through specialized water channel proteins called aquaporin (AQP) in various cells of animals, plants and microorganisms. In mammals eleven isoforms of AQP have been identified (AQP0–AQP10: King & Agre, 1996; Yamamoto & Sasaki, 1998; Ishibashi, Kuwahara & Sasaki, 2000; Hatakeyama et al., 2001). Aquaporins form membrane pores selectively permeable to water and, isoform-dependently, to some small solutes such as glycerol and urea. Several AQP isoforms such as AQP1 display ubiquitous tissue distribution, whereas other AQP isoforms display tissue-specific expression, for example, AQP0 (originally named MIP26) in the eye lens (Gorin et al., 1984), AQP2 in the apical plasma membrane (Fushimi et al., 1993) and AQP3 in the basolateral membrane (Echevarria et al., 1994; Ishibashi et al., 1994; Ma et al., 1994) of the kidney collecting duct, respectively. Amphibians possess a specialized region in the ventral skin which, compared to other tetrapods, is highly permeable to water and salts as well as to respiratory gases (Bentley & Main, 1972; Yorio & Bentley, 1977; Bentley & Yorio, 1979). Accordingly, water channels have been thought to exist in the ventral skin of amphibians. Indeed, for a long time, frog skin has been used as a useful model for investigating vasopressin regulation of transepithelial water permeability as well as urinary bladder (Brown et al., 1995). Freeze-fracture electron microscopical studies have suggested that intramembrane particles in amphibian urinary bladder and skin may be water channel protein because they translocate from their

cytoplasmic pools to plasma membrane after stimulation by vasopressin (Chevalier, Bourguet & Hugon, 1974; Kachadorian, Wade & DiScala 1975; Brown, Grosso & DeSousa, 1983). Recently, a cDNA encoding frog AQP has been cloned from the urinary bladder of *Rana esculenta* (Abrami et al., 1994) and *Bufo marinas* (Ma, Yang & Verkman, 1996), with high homology to mammalian AQP1. Furthermore, Ma's group noted three AQPs (Accession numbers: AAC69694 for AQP-t2, AF020622 for AQP-t3, and AAC69696 for AQP-t4) in the toad. However, there is no report regarding which AQPs are expressed in the ventral skin. In addition, amphibians exhibit various water-adaptation systems to maintain their water balance, because on land they are always exposed to the crisis of water loss by evaporation from the skin. Thus it is important to determine any correlation between tissue distribution of AQP isoforms and water adaptation in amphibians.

In this study we identified two types of cDNAs encoding amphibian AQP from the ventral pelvic skin of the tree frog, and discovered that one of them shows specific expression in principal cells in the pelvic skin.

Materials and Methods

Animals

Adult tree frogs (*Hyla japonica*) were captured in a field near our university, kept in laboratory conditions, and fed crickets. The ventral pelvic skins were removed under anesthesia with MS 222 (Nacalai tesque, Kyoto, Japan), and then processed for cDNA cloning and for immunohistochemical analysis. Similarly, several tissues from the frogs were used for experiments of mRNA expression.

Construction of the Frog Ventral Skin cDNA Library

Total RNA was prepared from 0.28 g of the skins using TRIZOL RNA extraction reagent (GibcoBRL, Rockville, MD). Then 11.52 μg of Poly (A) $^+$RNA was selected from about 572 μg of the total RNA using oligotex-dT30 super (Takara, Kyoto, Japan). We constructed a λZAP cDNA library (9.6×10^6 pfu/μg of arms) from the poly (A) $^+$RNA using a ZAP-express cDNA synthesis kit and a Gigapack III Gold cloning kit (Stratagene, La Jolla, CA), in accordance with the manufacturers' instructions.

Oligonucleotide Primers for Polymerase Chain Reaction (PCR)

Degenerate primers for the original amplification of frog AQP fragments were designed based on the amino-acid sequences around the two conserved NPA boxes of major intrinsic protein (MIP) family aquaporins (Agre, Brown & Nielsen, 1995). The following primers were commercially synthesized (Gibco BRL): P1 (sense): 5′-AGCGGGG(CG) (CT) CAC (AC) T (CT) AACCC-3′, P2 (antisense): 5′-GG (AT) CC (AG) A (CT) CCA (AG) AAGA (CT) CCA-3′, P3 (antisense): 5′-A (AG) (AG) GA (CG) C (GT) (GT) GC (AT) GG (AG) TTCAT-3′.

PCR Amplification

The skin poly (A) $^+$RNA (0.5 μg) was heated at 65°C for 3 min and quenched on ice. For cDNA synthesis, the denatured RNA was incubated in 20 μl reaction buffer containing RAV-2 reverse transcriptase (9.9 U, Takara), 1 mM dNTP, 7.5 mM oligo-dT (19) primer, and RNase inhibitor (20 U, Toyobo) at 42°C for 1 hr, and then at 52°C for 30 min. Using the reverse-transcribed first-strand cDNA, PCR was performed in 25 μl of Ex-Taq buffer containing 0.2 mM of each dNTP, 1 mM of primer P1 and 2 mM of primer P2 with 0.625 units of Ex-Taq polymerase (Takara). Nested PCR amplification was further performed using primers P1 and P3. The procedure of PCR amplification was an initial denaturation step of 95°C for 5 min, followed by denaturation (94°C, 90 sec), annealing (50°C, 90 sec) and extension (72°C, 150 sec) for 30 cycles in a thermal cycler (ASTEC, Fukuoka, Japan). Amplified fragments were subcloned into pGEM-3z vectors (Promega, Madison, WI), and sequenced. Since two clones with the sequences corresponding to Bufo AQP-t1 (AAC69693; Ma et al. 1996) and -t3 (AF020622) were identified, we tentatively designated them as AQP-h1 and AQP-h3, respectively.

Screening of the Frog Skin cDNA Library

DNA probes, obtained from the first PCR product as described above, were synthesized using a digoxigenin (DIG)-High Prime kit (Roche Mol. Biochem., Meylan, France) and used to screen the cDNA library of the pelvic skins, in accordance with the manufacturer's instructions. The membrane was hybridized with DIG-labeled cDNA probes at 68°C overnight and washed twice in 1× SSC/0.1% SDS for 1 hr at 50°C. After blocking, the membrane was incubated with alkaline phosphatase-conjugated sheep anti-DIG Fab antibody (Roche), reacted with 25 mM CSPD [Disodium 3-(4-methoxyspiro{1, 2-dioxetane-3, 2′-(5′-chloro)tricyclo[3.3.1.13.7] decan}-4-yl) phenyl phosphate) chemiluminescent substrate (Tropix, PE Applied Biosystems, Foster City, CA) and then exposed on Hyperfilm-ECL (Amersham Pharmacia Biotech, Buckinghamshire, UK).

DNA Sequence Analysis

The nucleotide sequence was analyzed by the dideoxy chain-termination method using a Thermo Sequenase Cycle Sequencing Kit (United States Biochemical, Cleveland, OH) with the Aloka DNA sequencing system (Model Lic-4200L(S), Aloka, Tokyo, Japan).

RT-PCR of *Hyla* Tissues

The tissue expression of AQP-h1 and AQP-h3 mRNAs was analyzed with RT-PCR. Total RNA was prepared using the TRIZOL reagent from the tree frog tissues (ventral pelvic skin, dorsal skin, urinary bladder, kidneys, brain, tongue, heart, lungs, liver, stomach, small intestine, large intestine, testes, ovaries and blood cells). After treatment of 20 μg total RNA with DNase I (4 U; Takara), a 10-μg aliquot of the total RNA was reverse transcribed in 20 μl of reaction buffer containing 1 mM of each dNTP, 9.9 U of RAV-2 reverse transcriptase (Takara), 20 U of RNase inhibitor (Toyobo), 7.5 mM of oligo-dT(19)primer (Gibco BRL), at 42°C for 1 hr, and then at 52°C for 30 min. RT-PCR was performed by the same method, basically as described above, using homologous primers: AQP-h1: P4 (sense), 5′-CGCCGCCATTATTTACGACT-3′ (678–697 b) and P5 (antisense), 5′-TGGTTTCATCTCCATGCGGG-3′ (791–810 b), AQP-h3: P6 (sense), 5′-TCGCGGCAACATTT TGCAAG-3′ (714–733 b) and P7 (antisense), 5′-TGGTCT-

GATGTATGTATGAG-3′ (939–958 b). The RT-PCR products were analyzed on a 2% agarose gel containing ethidium bromide (EtBr; 0.5 μg/ml) with Marker 6 (λ/Sty1 digest; Wako Pure Chemicals, Osaka, Japan) for molecular weight markers.

Southern Blot Analysis

To obtain cDNA probes, we performed the PCR using pBK-CMV plasmid vector containing AQP-h1 or AQP-h3 cDNAs, and primers P4 and P5 for AQP-h1 or primers P6 and P7 for AQP-h3 as described above. DIG-labeled cDNAs were synthesized with a DIG-High Prime kit (Roche). The membrane was subsequently hybridized with DIG-labeled cDNA probes, and then hybridization signals were detected with CSPD on Hyperfilm-ECL after incubating with alkaline phosphatase-labeled anti-DIG antibody, as described above.

Antibody

Oligopeptide corresponding to the C-terminal amino acids 255–271 (ST-141: SVGLNSVYSQTNSKKEKM) of the *Hyla* AQP-h3 was synthesized with a Model 433A (PE Applied Biosystems, Forster, CA). The antibody was raised in a rabbit using the ST-141 peptide coupled with Keyhole limpet hemocyanin (Pierce, Rockford, IL) as described previously (Tanaka, Nomizu & Kurosumi, 1991).

Western Blot Analysis

The ventral pelvic and back skins from the tree frogs were homogenized in cell lysis buffer [50 mM Tris-HCl (pH 8.0), 0.15 M NaCl, 1% Triton X-100, 0.1 mg/ml PMSF, 1 μg/ml aprotinin] and centrifuged in a microcentrifuge for 5 min to remove insoluble materials. The proteins were determined with a BCA Protein Assay Kit (Pierce, Rockford, IL). The supernatant protein (10 μg) was denatured at 70°C for 10 min in denaturation buffer comprising 2% SDS, 25 mM Tris-HCl, pH 7.5, 25% glycerol, and 0.005% bromophenol blue, subjected to electrophoresis on a 12% polyacrylamide gel, and then transferred to an Immobilon-P membrane (Millipore). The proteins in the membrane were reacted sequentially with anti-*Hyla* AQP-h3 serum diluted at 1:20,000, biotinylated anti-rabbit IgG (DAKO, Kyoto, Japan), and streptavidin-conjugated horseradish peroxidase (DAKO). The reaction product on the membrane was visualized using an ECL Western blot detection kit (Amersham). As a control, the primary antibody was replaced with anti-*Hyla* AQP-h3 serum preincubated with 10 μg/ml of the antigen peptide. In order to see whether the immunoreactive proteins were glycosylated, the extract from the ventral skins was treated for 1 hr at 37°C with peptide-*N*-glycosidase F (Daiichi Pure Chemicals, Tokyo, Japan) prior to SDS-PAGE and Western blotting.

Immunofluorescence

The skins were quickly removed, fixed for 4 hr in periodate-lysine-paraformaldehyde (PLP) fixative, dehydrated, and embedded in Paraplast. Sagittal 4-μm sections were cut and mounted on gelatin-coated slides. The deparaffinized sections were rinsed with distilled water and phosphate-buffered saline (PBS). For single labeling of *Hyla* AQP-h3, immunofluorescence staining was performed essentially as described previously (Tanaka et al. 1997). The sections were sequentially incubated with 1% bovine serum albumin-PBS, rabbit anti-*Hyla* AQP-h3 serum (1:10,000), and lissamine rhodamine sulfonyl chloride (LRSC)-labeled affinity-purified donkey anti-rabbit IgG (Jackson Immunoresearch, West Grove, PA). For nuclear counterstaining, 4′, 6-diamidino-2-phenylindole (DAPI) was included in the secondary antibody solution. The sections were washed with PBS and then mounted in PermaFluor (Immunon, Pittsburgh, PA). To check the specificity of the immunostaining, we performed an absorption test by preincubating the anti-AQP-h3 serum with C-terminal peptide (10 μg/ml) of AQP-h3 protein used as immunogen or with C-terminal peptide (10 μg/ml) of AQP-h1. Specimens were examined with an Olympus BX50 microscope equipped with a BX-epifluorescence attachment (Olympus Optical Co., Tokyo, Japan).

Osmotic Water Permeability of Oocytes

cRNAs were prepared from linearized pBK-CMV phagemid vectors containing the entire open reading frame of the AQP-h1 or AQP-h3 with XhoI (Takara) and transcribed/capped with T_3 RNA polymerase (mCAP^{TM} RNA Capping kit, Stratagene). Stage V and VI *Xenopus* oocytes were defolliculated by collagenase (1 mg/ml; Roche) and microinjected with cRNAs (5 or 50 ng) or water. After a 3-day incubation in Barth's buffer at 18°C, the oocytes were transferred from 200 mOsm to 70 mOsm Barth's buffer and osmotic volume increase was monitored at 24°C under an Olympus BX50 microscope with a 4× magnifying objective lens and a CCD camera connected to a computer. The coefficient of osmotic water permeability (*Pf*) was calculated from the initial slope of oocyte swelling according to the previously published method (Zhang, Logee & Verkman, 1990; Fushimi et al., 1993). In some experiments, $HgCl_2$ was added to a final concentration of 0.3 mM. To confirm whether AQP-h3 protein was expressed in *Xenopus* oocytes after injection of AQP-h3 cRNA, AQP-h3 cRNA-injected or water-injected oocytes were evaluated by Western blot analysis and immunostained as described above.

Results

cDNA cloning of *Hyla* AQP-h1

Figure 1*A* shows the full cDNA sequence of *Hyla* AQP-h1 and deduced amino acids. The cDNA consisted of a 5′-untranslated region of 115 bp and a 3′-untranslated region of 14 bp followed by a poly (A) tail. An open reading frame encoded a protein of 271 amino acids with a relative molecular mass calculated as 28,850 Da. Hydropathy analysis predicted six transmembrane regions with an N-terminus and a C-terminus localized in the cytoplasm similar to other MIP family members (Fig. 1*B*). The 3′-noncoding sequence contained a consensus polyadenylation signal (AATAAA) with a poly A tail. There was one putative N-linked glycosylation site at Asn-44 and two protein kinase C phosphorylation sites at Thr-161 and Thr-243 in the predicted amino-acid sequence of AQP-h1. The amino-acid sequence contained the conserved NPA motifs found in all MIP family members, as well as a cysteine just upstream from the second NPA motif, which confers mercurial sensitivity common to all the AQPs except AQP0, AQP4 and AQP7. The homology of amino-acid sequences between the *Hyla* AQP-h1 and Bufo AQP-t1 or *Rana* CHIP28 (AQP1), rat AQP1, mouse AQP1,

A

```
-115        AATTCGGCACGAGGCCCACTTTTCTAGGAGAGAACTTGAACAATTTAGATTTTTT -61
 -60  TTGTTTTTAATTTAAATTTAAATTTTTAAATTTTTAAGAAAAAAAAGTGAATTCAAGAAG  -1
   1  ATGGCCAGTGAATTCAAAAAGATGGCCTTCTGGAGGGCGGTGATCGCCGAGTTCTTGGCC  60
   1   M  A  S  E  F  K  K  M  A  F  W  R  A  V  I  A  E  F  L  A   20

  61  ATGATCATGTTCGTTTTTATAAGTATCGGCGCCGCTCTCGGCTTCAACTTCCCCATCCAA 120
  21   M  I  M  F  V  F  I  S  I  G  A  A  L  G  F  N  F  P  I  Q   40

 121  GAGAAGACCAACGAGACCGTCGGCCGGACGCAGGACATCGTCAAGGTGTCCCTGGCTTTC 180
  41   E  K  T  N  E  T  V  G  R  T  Q  D  I  V  K  V  S  L  A  F   60
             ▲                                    primer1
 181  GGGCTGTCCATCGCCACCATGGCGCAGAGCGTGGGGCACATCAGCGGAGCCCACCTCAAC 240
  61   G  L  S  I  A  T  M  A  Q  S  V  G  H  I  S  G  A  H  L  N   80

 241  CCCGCCGTCACCCTGGGCTGCCTCCTCAGCTGTCAGATCAGCATCCTAAAGGCCGTTATG 300
  81   P  A  V  T  L  G  C  L  L  S  C  Q  I  S  I  L  K  A  V  M  100

 301  TACATCATCGCGCAGTGCCTGGGCGCCGTGGTCGCCACCGCCATCTTGTCCGGCATCACC 360
 101   Y  I  I  A  Q  C  L  G  A  V  V  A  T  A  I  L  S  G  I  T  120

 361  AGCAACCTGGCGGGCAACACGCTCGGGCTGAATGGGCTGAGTAACGGGGTGACGGCCGGG 420
 121   S  N  L  A  G  N  T  L  G  L  N  G  L  S  N  G  V  T  A  G  140

 421  CAGGGTCTGGGGGGTGGAGATCATGGTCACGTTCCAGCTGGTCCTCTGCGTTGTTGCGGTC 480
 141   Q  G  L  G  G  V  E  I  M  V  T  F  Q  L  V  L  C  V  V  A  V  160

 481  ACAGACAGAAGACGACGCGATGTCTCGGGGTCCGTTCCTCTGGCCATAGGACTCTCTGTT 540
 161   T  D  R  R  R  R  D  V  S  G  S  V  P  L  A  I  G  L  S  V  180
       ◆                                    primer3
 541  GCCCTAGGACATCTCATTGCGATCGATTACACTGGGTGCGGTATGAACCCTGCAAGGTCT 600
 181   A  L  G  H  L  I  A  I  D  Y  T  G  C  G  M  N  P  A  R  S  200
                                        △ primer2
 601  TTCGGTTCTGCAGTAGTCGCTAAAAACTTCCAGTATCACTGGATCTTCTGGGTTGGACCA 660
 201   F  G  S  A  V  V  A  K  N  F  Q  Y  H  W  I  F  W  V  G  P  220

 661  ATGATCGGAGGAGCAGCCGCCGCCATTATTTACGACTTCATCTTAGCGCCACGAACCAGC 720
 221   M  I  G  G  A  A  A  A  I  I  Y  D  F  I  L  A  P  R  T  S  240

 721  GACTTGACAGACCGCCTAAAGGTCTGGACCAACGGACAGGTGGAGGAGTACGAGCTGGAC 780
 241   D  L  T  D  R  L  K  V  W  T  N  G  Q  V  E  E  Y  E  L  D  260
          ◆
 781  GGGGAAGACGCCCGCATGGAGATGAAACCAAAATAA                        816
 261   G  E  D  A  R  M  E  M  K  P  K  *                         271

 817  AGAAGAGTAATAAAAAAAAAAAAAAAAA                                847
```

B

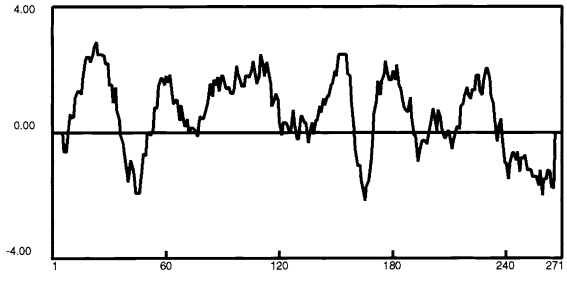

Fig. 1. (*A*) Nucleotide and deduced amino-acid sequences of frog AQP-h1 cDNA. The predicted amino acid is shown below the nucleotide sequence. The asterisk indicates the termination codon. Solid triangles indicate putative N-glycosylation sites. NPA motifs and polyadenylation signal regions are outlined. Diamonds and white triangles indicate phosphorylation sites for protein kinase C and mercurial-inhibition sites, respectively. (*B*) Kyte-Doolittle hydropathy profile (window 11) of the deduced AQP-h1 amino-acid sequence.

or human AQP1 was 89.3, 91.2, 75.1, 76.2, and 75.8%, respectively.

cDNA cloning of *Hyla* AQP-h3

Figure 2*A* shows the full cDNA sequence of *Hyla* AQP-h3 and deduced amino acids. The cDNA consisted of a 5′-untranslated region of 49 bp and a 3′-untranslated region of 565 bp followed by a poly (A) tail. An open reading frame encoded a protein of 271 amino acids with a relative molecular mass calculated as 29,204 Da. Hydropathy analysis predicted six transmembrane regions with an N-terminus and a C-terminus localized in the cytoplasm similar to other MIP family members (Fig. 2*B*). The 3′-noncoding sequence contained a consensus polyadenylation signal (ATTAAA) with a poly A tail. There were two putative N-linked glycosylation sites at Asn-124 and Asn-125, two protein kinase C phosphorylation sites at Ser-152 and Ser-232, and one protein kinase A phosphorylation site at Ser-255 in the predicted amino-acid sequence of AQP-h3. The amino-acid sequence contained the conserved NPA motifs found in all MIP family members, as well as a cysteine just upstream from the second NPA motif, which is similar to *Hyla* AQP-h1. *Hyla* AQP-h3 had the highest amino acid sequence homology to *Bufo* AQP-t3 (86.8%) and high homology to rat AQP2 (56.8%), mouse AQP2 (57.1%) and human AQP2 (58.2%), but less homology to rat AQP3 (27.5%), mouse AQP3 (28.5%) and human AQP3 (28.2%).

Expression Distribution of *Hyla* AQP mRNAs in Various Tissues

To investigate tissue distribution of *Hyla* AQP mRNA expressions, RT-PCR was performed using total RNA from various tissues. AQP-h1 mRNA was observed in most tissues except blood cells and liver, whereas AQP-h3 mRNA was detected only in the ventral skin (Fig. 3). This RT-PCR result was confirmed by Southern blot analysis.

Antibody Specificity

To test the specificity of the antiserum toward the *Hyla* skins, we conducted Western blot analysis of their extracts. In the extract of ventral pelvic skin, the antiserum detected a major band at 29.0 kDa and a minor smear band between 35.9 and 45.2 kDa. No band was detectable in the dorsal skin extract (Fig. 4*A*). The bands described above were not detected when anti-*Hyla* AQP-h3 was preabsorbed with the peptide used as the immunogen (Fig. 4*B*). To confirm that the immunoreactive bands are glycosylated, we performed a digestion experiment using peptide-*N*-glycosidase F. After digestion, the stained smear band became a band of 29.0 kDa, suggesting that the bands of apparent higher molecular mass represented glycosylated forms of the 29.0-kDa *Hyla* AQP-h3 protein (Fig. 4*C*).

Localization of *Hyla* AQP-h3 in the Epidermis

The *Hyla* epidermis is organized into four successive layers: the stratum corneum, the granulosum, the spinosum, and the germinativum. The layers consist of two main cell types: principal cells and mitochondria-rich cells. In some sections, exocrine glands were observed. When the ventral epidermis was stained by the immunofluorescence method, AQP-h3 protein was detected in two or three layers of the stratum granulosum, located just beneath the stratum corneum (Figs. 5*A*, *B*). In the principal cells, AQP-h3 was localized in the entire plasma membrane. AQP-h3 was also found in the cytoplasm as a spot-like pattern, suggesting that AQP-h3 may be pooled in the cytoplasm (Fig. 5*C*). No signal was found in other types of cells including the mitochondria-rich cells and exocrine glandular cells in the pelvic skin (Figs. 5*A*, *B*). To confirm the specificity of the staining, we carried out a control experiment.

Immunopositive labeling for AQP-h3 in the principal cells was abolished when the antiserum was preincubated with the C-terminal peptide of *Hyla* AQP-h3 protein used as immunogen (Fig. 5*D*). On the other hand, the addition of C-terminal peptide of *Hyla* AQP-h1 did not affect the AQP-h3 labeling (*data not shown*). When the junction region between the pelvic and pectral skins in the ventral side was immunostained with the antiserum, the labeling intensity gradually decreased toward the pectral from the pelvic skin, suggesting that the AQP-h3 protein is only expressed in the pelvic skin (Figs. 5*E*, *F*). In addition, the dorsal skin did not express the AQP-h3 protein (Figs. 5*G*, *H*).

Expression of *Hyla* AQP-h3 in *Xenopus* oocytes

Transmembrane water flow through the Hyla AQP-h1 and AQP-h3 protein was evaluated by expression in *Xenopus* oocytes. After 3 days of incubation at 18°C, the oocytes were transferred from isotonic (200 mOsm) to hypoosmotic (70 mOsm) Barth's solution: swelling was monitored by a microscope with attached CCD camera, and the coefficient of osmotic water permeability (*Pf*) was calculated (Fig. 6*A*). The *Pf* of AQP-h1-injected oocytes was approximately 18 times higher than that of water-injected oocytes. The stimulated water permeability was inhibited by 0.3 mM $HgCl_2$ by 48% (Fig. 6*B*). On the other hand, swelling of AQP-h3 cRNA-injected oocytes appeared higher than that of water-injected oocytes, but no significant difference was observed between them. To

A

```
-49                AATTCGGCACGAGGGTTTTGAGTCTCCTTAACTTTTATAGACTGTAATC   -1
  1 ATGCTTAAGGAGCTATGCGCAGGATTTAATTTTAAGGCATTTCTAGCTGAGCTGATAGCA    60
  1  M  L  K  E  L  C  A  G  F  N  F  K  A  F  L  A  E  L  I  A    20

 61 ACCCTTGTCTTTGTATTTGTTGGCCTGGGCTCAACGCTATCATGGACGGGGGCTCTCCCA   120
 21  T  L  V  F  V  F  V  G  L  G  S  T  L  S  W  T  G  A  L  P    40

121 ACTGTCTTACAAATAGCCTTCACTTTTGGCTTGGGAATAGGTACAATGGTACAAGCTGTA   180
 41  T  V  L  Q  I  A  F  T  F  G  L  G  I  G  T  M  V  Q  A  V    60
                primer1
181 GGTCACATCAGTGGGGCCCATATCAACCCTGCTGTAACTATAGCACTGCTTGTTGGGGCC   240
 61  G  H  I  S  G  A  H  I  N  P  A  V  T  I  A  L  L  V  G  A    80

241 CGAATTTCTCTGATCCAGACAGTTTTCTATGTGATTGCTCAGATGCTGGGAGCAGTGATA   300
 81  R  I  S  L  I  Q  T  V  F  Y  V  I  A  Q  M  L  G  A  V  I   100

301 GGAGCTGCTTTGCTGTATGAGTTTTCACCATCTGACATCCGGGGAGGTTTTGGAGTGAAC   360
101  G  A  A  L  L  Y  E  F  S  P  S  D  I  R  G  G  F  G  V  N   120

361 CAGCCGAGCAACAATACAAGTCCTGGACAAGCAGTCGCGGTAGAAATTATTCTTACAATG   420
121  Q  P  S  N  N  T  S  P  G  Q  A  V  A  V  E  I  I  L  T  M   140
          ▲  ▲
421 CAACTGGTCCTATGCATCTTTGCTACAACAGACAGCCGGAGGACAGACAACATCGGGTCT   480
141  Q  L  V  L  C  I  F  A  T  T  D  S  R  R  T  D  N  I  G  S   160
                                      ◆
481 CCAGCCATATCTATAGGACTGTCAGTGGTACTGGGACACTTACTTGGCATTTACTACACT   540
161  P  A  I  S  I  G  L  S  V  V  L  G  H  L  L  G  I  Y  Y  T   180
             primer3
541 GGATGTTCAATGAATCCTGCACGGTCCTTTGGTCCAGCTTTGATAACAGGAAATTTCGAA   600
181  G  C  S  M  N  P  A  R  S  F  G  P  A  L  I  T  G  N  F  E   200
        △ primer2
601 TACCACTGGATTTTCTGGGTGGCGCCAATAACCGGAGCAATCTTCGCATGCTTGATTTAT   660
201  Y  H  W  I  F  W  V  A  P  I  T  G  A  I  F  A  C  L  I  Y   220

661 GACTATATCTTTGCCCCTCAATTCATAAGCCCCAGCGAGAGACTCGAAATCCTTCGTGGC   720
221  D  Y  I  F  A  P  Q  F  I  S  P  S  E  R  L  E  I  L  R  G   240
                                      ◆
721 AACATTTTGCAAGAGAACGAAAAAGAAGAGAGACGAAAACAATCTGTAGGCCTCAATTCT   780
241  N  I  L  Q  E  N  E  K  E  E  R  R  K  Q  S  V  G  L  N  S   260
                                         ■
781 GTTTACAGTCAAACAAATAGCAAAGAAAAAATGTGA                          816
261  V  Y  S  Q  T  N  S  K  E  K  M  *                          271

817 AATTCTATTTTGTATTTTTTTTTTGTGTTGCGAGGATATtGTACAGAGATGTTATGAACG  876
877 GGCCAATAGATTGGTTACTGGTTCTATGGGTTTTCGAACCTGATAATTGTACTGCTATCA  936
937 AACTCATCCATACATCAGACCATGACGATTGTTTTATTTTTGTTTTTTAACAAAACACTA  996
997 TGCATGTATTTTTTACATAATGTATATTTTATTATTGATTTTGTGACACTTAAAAAATTG 1056
1057 TATAAAATTAGAAAGCTATGGCTGCTTTCTACTAGAAACAGCACCACACTTGTCCTTTGG 1116
1117 CCATACTTGTCATAGACATATTCTTTAAGATGACTCCCAGTTAATGTGACAGTAGCTTTT 1176
1177 ACAGTGCACACATTTGTTTATAGAGAAAGATAAGGTCAATTGGTCTTGTGTATTATAGTG 1236
1237 TATATATTAGGATGTTAAGAATACCTATTGTCAGATTCTAACAACCTGAATATTGTGATT 1296
1297 TATACCCATTAAATAGTGAGGTCACCTTTGAACATCTTGTTCCAGTTTTTATATGAAGCT 1356
1357 TCAGTAAATTTTGTAAATATATTCTAAAAAAAAAAAAAAAAAAAAAA              1404
```

B

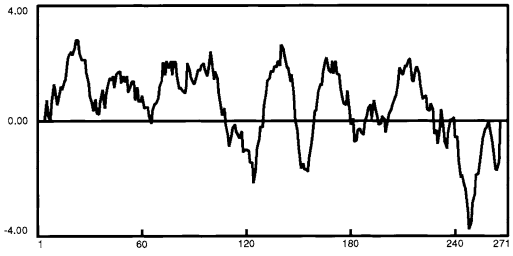

Fig. 2. (*A*) Nucleotide and deduced amino-acid sequences of frog AQP-h3 cDNA. The predicted amino acid is shown below the nucleotide sequence. The asterisk indicates the termination codon. Solid triangles indicate putative N-glycosylation sites. NPA motifs and polyadenylation signal regions are outlined. Diamonds, squares and white triangles indicate phosphorylation sites for protein kinase C and for protein kinase A, and mercurial-inhibition sites, respectively. (*B*) Kyte-Doolittle hydropathy profile (window 11) of the deduced AQP-h3 amino-acid sequence.

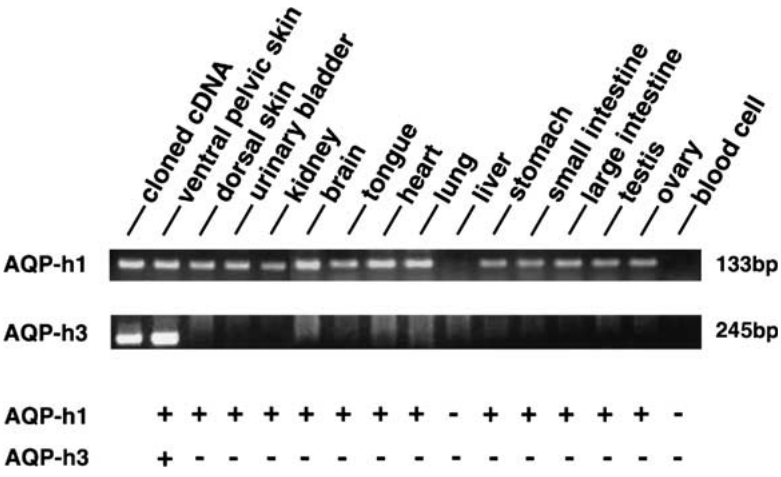

Fig. 3. RT-PCR of *Hyla* tissue extracts. RT-PCR products using primers as described in Materials and Methods were separated on a 2% agarose gel and stained with ethidium bromide.

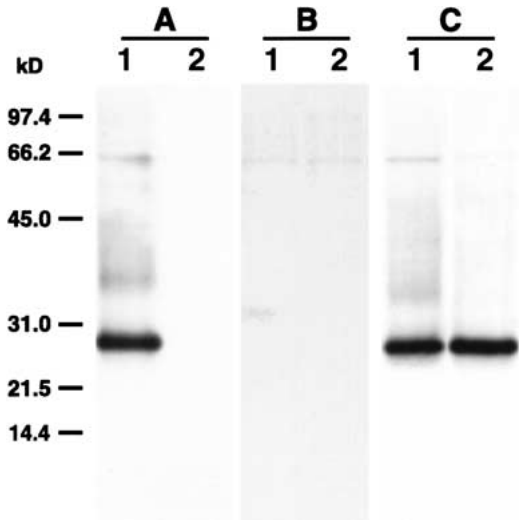

Fig. 4. Characterization of anti-AQP-h3 serum by Western blot analysis. (*A*) Immunoreactive bands are seen at 29.0 kDa and at 35.9–45.2 kDa in an extract of ventral pelvic skin (lane *1*). No bands are visible in the extract of dorsal skin (lane *2*). (*B*) The membrane was immunostained with the antiserum preabsorbed with the antigen peptide (10 μg/ml). Immunoreactive bands were completely eliminated except for the bands at about 66.2 kDa, suggesting that this band is nonspecific. (*C*) Western blot analysis of extracts before and after digestion of the extracts by peptide-*N*-glycosidase F. Specific bands with the extract of ventral skin (lane *1*) seen before digestion are replaced by a single band of 29.0 kDa, presumed to be the nonglycosylated form of *Hyla* AQP-h3. Lane *2* corresponds to the ventral skin extract after digestion.

evaluate whether AQP-h3 protein was expressed in the AQP-h3-injected oocytes, we performed a Western blot analysis on the extract of the oocytes. As shown in Fig. 6*C*, the AQP-h3 protein was detected as one band at 29 kDa (lane *1*), which was consistent with the molecular weight of the AQP-h3 detected in the ventral skins (lane *3*). In addition, the antiserum pre-absorbed with the antigen peptide stained no band (lane *2*). However, when sections of the AQP-h3 cRNA-injected oocytes were immunostained with anti-*Hyla* AQP-h3, punctate immunofluorescence was seen in the cytoplasm, but not in the plasma membranes (Fig. 6*D-a*, *b*). The immunopositive labeling was completely eliminated by preabsorption of the antiserum with 10 μg/ml of the antigen peptide (Fig. 6*D-c*) and no immunolabeling was seen in water-injected oocytes (Fig. 6*D-d*).

Discussion

The present study describes the full sequences of mRNAs encoding two different types of AQPs from frog skin. Both of the two AQPs, AQP-h1 and AQP-h3, were structurally characterized by having two NPA motifs and six putative transmembrane domains as well as a cysteine at a mercurial sensitivity site just upstream from the second NPA motif. From a homology analysis, the deduced amino-acid sequences of *Hyla* AQP-h1 showed higher homology to mammalian AQP1, and those of *Hyla* AQP-h3 to mammalian AQP2 than to mammalian AQP3. Furthermore, AQP-h3 had a putative phosphorylation site by protein kinase A at Ser-255, identical to that of mammalian AQP2 (Brown, Katsura & Gustafson, 1998). Thus, these data suggest a possibility that AQP-h3 translocates from the cytoplasmic pools to plasma membrane by vasotocin (the counterpart of vasopressin in non-mammalian vertebrates).

In this study, we investigated the expression of the two AQP mRNAs using RT-PCR. AQP-h1 was expressed in a wide variety of tissues, whereas AQP-h3 was observed only in the ventral skin. Taken together with the data from sequence homology between AQP-h1 and mammalian AQPs, it is very likely that AQP-h1 is a counterpart of mammalian AQP1. However, there was one point of difference: mammalian AQP1 is abundantly expressed in red blood cells, but AQP-h1 is absent in the cells. In mammals, red blood cells are thought to need water perme-

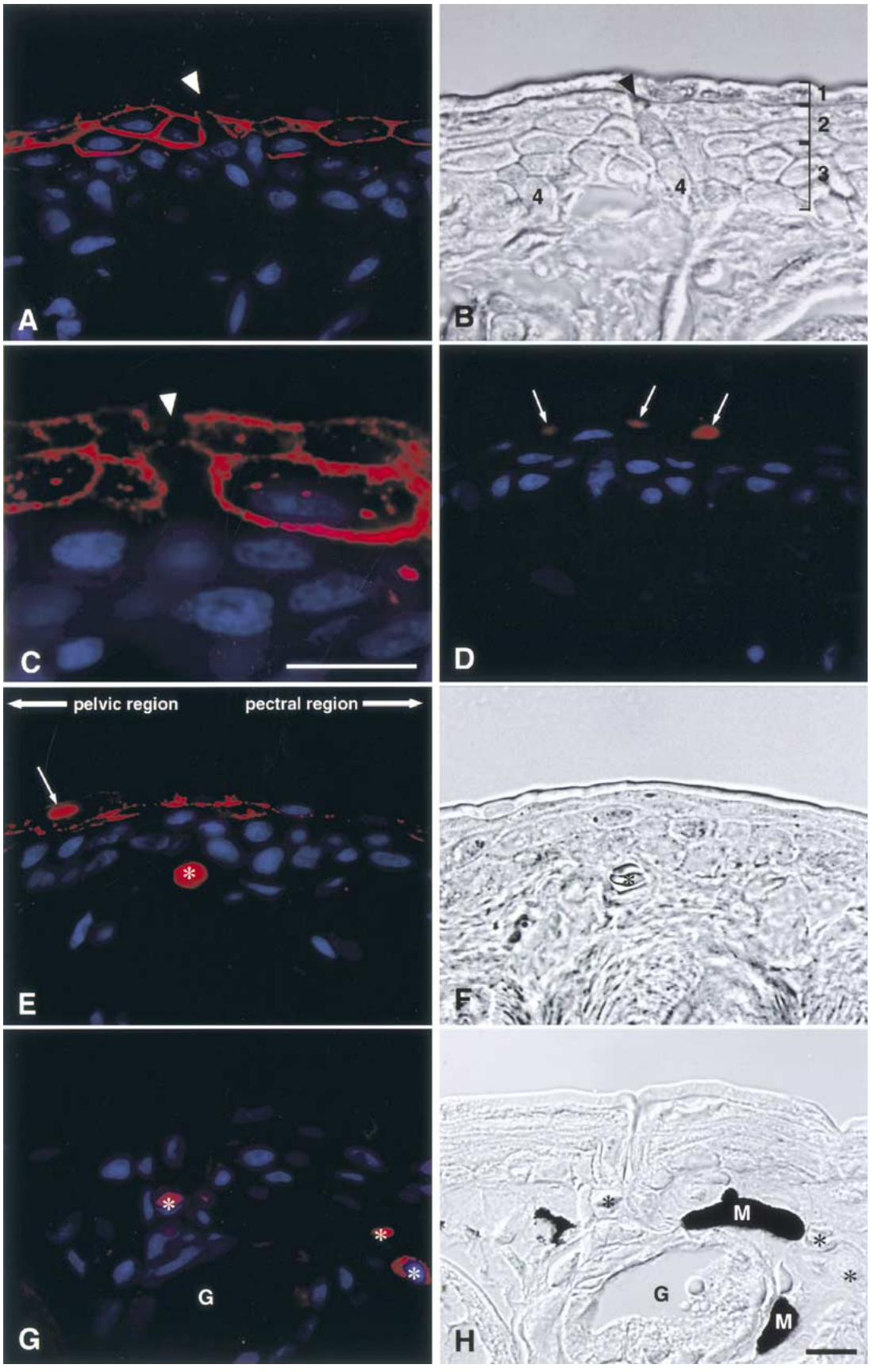
A
B
1
2
3
4
4
C
D
pelvic region
pectral region
E
F
G
G
H
G
M
M

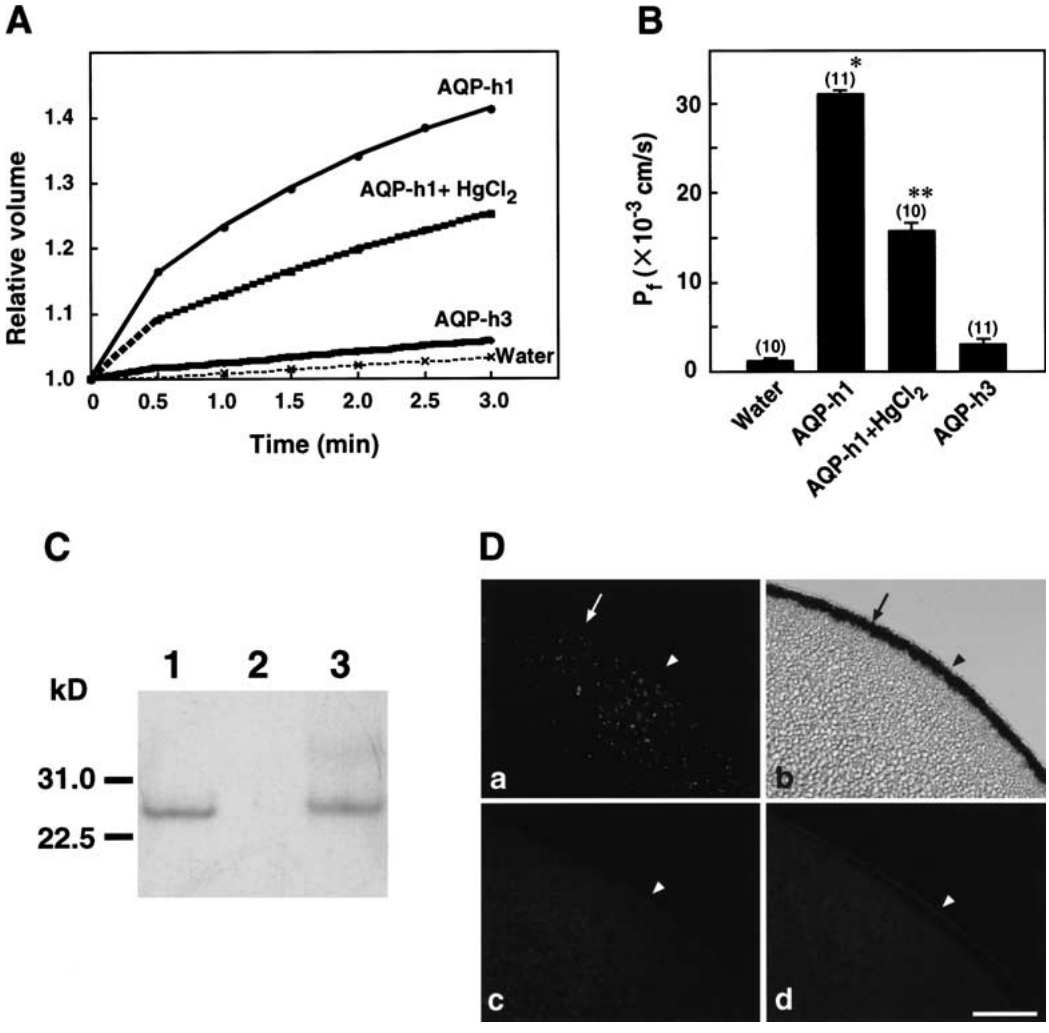

Fig. 6. Expression of AQP-h1 and AQP-h3 in *Xenopus* oocytes. (*A*) Time course of the osmotic swelling. Oocytes were microinjected with water or cRNAs encoding AQP-h1 (5ng) or AQP-h3 (50ng). Some AQP-h1-injected oocytes were incubated with 0.3 mM $HgCl_2$. (*B*) Osmotic water permeability (*Pf*) was calculated from the initial rate of oocyte swelling. All data shown are mean ± SE of measurements from 10–11 oocytes in each experimental group. $^{*}P < 0.001$ *vs.* water, $^{**}P < 0.001$ *vs.* AQP-h3. (*C*) Western blot analysis of AQP-h3-injected oocytes using anti-AQP-h3. Immunoreactive band is seen at 29.0 kDa in an extract of the AQP-h3-injected oocytes (lane *1*) after completion of the swelling experiments. In the water-injected oocytes, no bands are detected with the antibody (lane *2*). In addition, the 29-kDa band is consistent with that detected in the extract of ventral skins (lane *3*). (*D*) Immunofluorescence images for AQP-h3 protein in AQP-h3-injected oocytes. (*a*) After completion of swelling experiments, immunoreactive AQP-h3 materials are punctately seen in the cytoplasm, but not in the plasma membrane. (*b*) The corresponding Nomarski differential interference image. (*c*) In the absorption test, positive immunoreactive materials obtained with anti-AQP-h3 are nearly eliminated at background levels in the AQP-h3-injected oocyte. (*d*) Similarly, only background levels are seen in the water-injected oocyte with anti-AQP-h3. Arrows and arrowheads indicate pigment layer and plasma membrane, respectively. Bar = 50 μm.

Fig. 5. Immunofluorescence localization of AQP-h3 in the ventral pelvic skin. Fluorescence images for AQP-h3 (*A*, *C*, *D*, *E*, *G*) and corresponding Nomarski differential interference contrast images (*B*, *F*, *H*) are shown. AQP-h3 is present in a few layers of the stratum granulosum just beneath the stratum corneum. (*B*) The epidermis consists of four layers: the stratum corneum (*1*), the granulosum (*2*), the spinosum (*3*), and the germinativum (*4*). (*C*) Enlarged view of AQP-h3-positive principal cells in the stratum granulosum. The punctate label is seen throughout the entire region of the plasma membranes and in the cytoplasm. (*D*) No labeling was detected in any cells of the pelvic skins when anti-AQP-h3 was preabsorbed with the corresponding antigen peptide. Nonspecific labels are seen in the nucleus of the stratum corneum (*arrows*). (*E*, *F*) The labeling intensity for AQP-h3 gradually decreases towards the pectral from the pelvic skin. (*G*, *H*). None of the cells in dorsal skin are labeled with anti-AQP-h3. The asterisk corresponds to red blood cells, displaying a nonspecific label for AQP-h3. *Triangle*: mitochondria-rich cells, *M*: melanin granules, *G*: exocrine gland. Bar: *A*, *B*, *D*, *E*, *F*, *G* = 10 μm, *C* = 10 μm.

ability to survive transit through the renal medulla, where the interstitial osmolality is very high (King & Agre, 1996). In amphibians, on the other hand, nephrons do not develop Henle's loops as in mammals, so they are unable to concentrate urea (Acher, Chauv &Rouille, 1997), which suggests that the osmotic gradient in the frog kidney is low. Accordingly, the lack of AQP-h1 mRNA expression in the frog blood cells may be expected.

Western blot analysis of the extracts of *Hyla* skin showed one major band at 29.0 kDa and a smear band between 35.9 and 45.2 kDa. The 29.0-kDa band was consistent with the molecular mass predicted from the amino-acid sequence of *Hyla* AQP-h3. The smear band was presumed to be glycosylated forms of *Hyla* AQP-h3 with a different number of sugar side chains, because *Hyla* AQP-h3 has two potential N-glycosylation sites. Digestion experiments with peptide-*N*-glycosidase F revealed a single band of 29.0 kDa, a value close to the molecular mass (29,204 Da) calculated from the amino-acid sequence of AQP-h3. Furthermore, the present Western blot analysis using the preabsorbed antiserum confirmed that these immunoreactive bands were specific to the antiserum.

In this immunofluorescence study, we revealed that AQP-h3 is specifically expressed in the plasma membranes of principal cells in ventral pelvic skin. This immunopositive labeling was in good agreement with the results of the tissue distribution of mRNA by RT-PCR. Therefore, AQP-h3 is thought to play a pivotal role in absorbing water in pelvic skin. We also demonstrated that the expression of AQP-h3 protein gradually increased as the cell differentiated and moved upward to the surface, reaching a maximum in the principal cells in the outermost layer of the stratum granulosum, and then completely disappearing in the stratum corneum. Identification of the actual sites of water influx in the pelvic skin cells is of interest and importance to gain an understanding of the regulation of water balance in the frog. It is well accepted that tight junctions between cells play a role in blocking the diffusion of water and solutes. Electron microscopical studies have reported that tight junctions are found between adjoining cells in the stratum corneum and in the outermost layer of the stratum granulosum in the frog skin (Farquhar & Palade, 1965, Brown & Ilic, 1979), but not in lower levels of the epidermis (Brown, Grosso & DeSousa, 1983). The present immunohistochemical study strongly suggests that water passes through transcellular paths via AQP-h3 at the outermost principal cells of the stratum granulosum in the ventral skin, and afterwards through intercellular spaces in the region from the lower layer of the stratum granulosum to the small blood vessels in the connective tissue. We were unable to stain the plasma membranes of the stratum corneum using the AQP-h3 antiserum; the reason for this is unclear. However, the stratum corneum is generally considered to be water-permeable.

In the present osmotic water-permeability experiments using *Xenopus* oocytes, we demonstrated that AQP-h1 facilitates water permeability, whereas weak water permeability was observed in the AQP-h3-injected oocytes. Concerning the AQP-h3-injected oocytes, our Western blot analysis and immunohistochemistry revealed that AQP-h3 protein did not fully translocate to plasma membrane in the ooctyes, thereby causing low activity of AQP-h3 in water permeability assays. On the other hand, as mentioned above, the present immunohistochemical observation on *Hyla* ventral skin cells provided an important evidence showing the presence of AQP-h3 protein in plasma membrane: AQP-h3 protein is able to travel to plasma membrane in skin cells in situ. Therefore, our results led to a possibility that vasotocin-regulated membrane trafficking mechanisms or unknown factors, which may exist in *Hyla* ventral skin cells, but not in *Xenopus* oocytes, is necessary for the AQP-h3 protein to translocate to plasma membrane. Fushimi et al. (1993) had also noted that the *Pf* value in AQP-2 (WCH-CD)-injected oocytes was lower than that reported for AQP1 (CHIP28)-injected oocytes and they pointed out a possibility that the reduced surface expression of the AQP-2 in oocytes is due to a lack of vasopressin-regulated membrane trafficking mechanisms. In addition, the deduced amino-acid sequence of *Hyla* AQP-h3 showed a higher homology with that of mammalian AQP family members. Taken together, these data suggest that *Hyla* AQP-h3 could be classified into a member of the AQP family. Further studies will be needed to clarify the reason why the AQP-h3 protein does not translocate to plasma membrane in *Xenopus* oocytes.

As mentioned above, frog pelvic skin has a higher permeability to water compared with other tissues. Furthermore, the water permeability in the skin is enhanced after stimulation by vasotocin from the pars nervosa (Acher, Chauvet & Rouille, 1997). Accordingly, it is thought that there are two systems for water absorption in the ventral skin: constitutive and regulated systems (Yorio & Bentley, 1977). *Hyla* AQP-h3 has a putative phosphorylation site at Ser-255, but AQP-h3 is expressed in the apical and basolateral plasma membranes of the principal cells. This finding is in contrast with evidence that mammalian AQP2 is localized in the apical membranes of the principal cells of the kidney collecting duct, and that its expression increases in response to vasopressin stimulation (Sasaki, Ishibashi & Marumo, 1998). In amphibians, it has been established that there are three water-reabsorption regions regulated by vasotocin: the pelvic skin, the urinary bladder and the kidneys. Therefore, vasotocin-dependent AQP should be expressed in these tissues. In our preliminary study, we obtained another cDNA encoding *Hyla*

AQP-h2, which is expressed in several tissues including the urinary bladder, kidney and pelvic skin of the frogs, suggesting that this AQP may be regulated by vasotocin. However, the exact localization and regulation of *Hyla* AQP-h2 is unclear. Taken together, it is suggested that *Hyla* AQP-h3 is involved in the constitutive water absorption of the pelvic skin.

This work was supported in part by a Grant-in-Aid for Scientific Research from the Ministry of Education, Science, Sports, and Culture of Japan to ST.

References

Acher, R., Chauvet, J., Rouille, Y. 1997. Adaptive evolution of water homeostasis regulation in amphibians: vasotocin and hydrins. *Biol. Cell* **89:**283–291

Abrami, L., Simon, M., Rousselet, G., Berthonaud, V., Buhler, J.M., Ripoche, P. 1994. Sequence and functional expression of an amphibian water channel, FA-CHIP: a new member of the MIP family. *Biochim. Biophys. Acta* **1192:**147–151

Agre, P., Brown, D., Nielsen, S. 1995. Aquaporin water channels: unanswered questions and unresolved controversies. *Curr. Opin. Cell Biol.* **7:**472–483

Bentley, P.J., Main, A.R. 1972. Zonal differences in permeability of the skin of some anuran Amphibia. *Am. J. Physiol.* **223:**361–363

Bentley, P.J., Yorio, T. 1979. Do frogs drink? *J. Exp. Biol.* **79:**41–46

Brown, D., Ilic, V. 1979. Freeze fracture differences in plasma membranes of the stratum corneum and replacement layer cells of amphibian epidermis. *J. Ultrastruct. Res.* **67:**55–64

Brown, D., Grosso, A., DeSousa, R.C. 1983. Correlation between water flow and intramembrane particle aggregates in toad epidermis. *Am. J. Physiol.* **245:**C334–C342

Brown, D., Katsura, T., Kawashima, M., Verkman, A.S., Sabolic, I. 1995. Cellular distribution of the aquaporins: a family of water channel proteins. *Histochem. Cell Biol.* **104:**1–9

Brown, D., Katsura, T., Gustafson, C.E. 1998. Cellular mechanisms of aquaporin trafficking. *Am. J. Physiol.* **275:**F328–F331

Chevalier, J., Bourguet, J., Hugon, J.S. 1974. Membrane associated particles: distribution in frog urinary bladder epithelium at rest and after oxytocin treatment. *Cell Tissue Res.* **152:**129–140

Echevarria, M., Windhager, E.E., Tate, S.S., Frindt, G. 1994. Cloning and expression of AQP3, a water channel from the medullary collecting duct of rat kidney. *Proc. Natl. Acad. Sci. USA* **91:**10997–11001

Farquhar, M.G., Palade, G.E. 1965. Cell junctions in amphibian skin. *J. Cell Biol.* **26:**263–291

Fushimi, K., Uchida, S., Hara, Y., Hirata, Y., Marumo, F., Sasaki, S. 1993. Cloning and expression of apical membrane water channel of rat kidney collecting tubule. *Nature* **361:**549–552

Gorin, M.B., Yancey, S.B., Cline, J., Revel, J.P., Horwitz, J. 1984. The major intrinsic protein (MIP) of the bovine lens fiber membrane: characterization and structure based on cDNA cloning. *Cell* **39:**49–59

Hatakeyama, S., Yoshida, Y., Tani, T., Koyama, Y., Nihei, K., Ohshiro, K., Kamiie, J.I., Yaoita, E., Suda, T., Hatakeyama, K., Yamamoto, T. 2001. Cloning of a new aquaporin (AQP10) abundantly expressed in duodenum and jejunum. *Biochem. Biophys. Res. Commun.* **287:**814–819

Ishibashi, K., Sasaki, S., Fushimi, K., Uchida, S., Kuwahara, M., Saito, H., Furukawa, T., Nakajima, K., Yamaguchi, Y., Gojobori, T., Marumo, F. 1994. Molecular cloning and expression of a member of the aquaporin family with permeability to glycerol and urea in addition to water expressed at the basolateral membrane of kidney collecting duct cells. *Proc. Natl. Acad. Sci. USA* **91:**6269–6273

Ishibashi, K., Kuwahara, M., Sasaki, S. 2000. Molecular biology of aquaporins. *Rev. Physiol. Biochem. Pharmacol.* **141:**1–32

Kachadorian, W.A., Wade, J.B., DiScala, V.A. 1975. Vasopressin: induced structural change in toad bladder luminal membrane. *Science* **190:**67–69

King, L.S., Agre, P. 1996. Pathophysiology of the aquaporin water channels. *Annu. Rev. Physiol.* **58:**619–648

Ma, T., Frigeri, A., Hasegawa, H., Verkman, A.S. 1994. Cloning of a water channel homolog expressed in brain meningeal cells and kidney collecting duct that functions as a stilbene-sensitive glycerol transporter. *J. Biol. Chem.* **269:**21845–21849

Ma, T., Yang, B., Verkman, A.S. 1996. cDNA cloning of a functional water channel from toad urinary bladder epithelium. *Am. J. Physiol.* **271:**C1699–C1704

Sasaki, S., Ishibashi, K., Marumo, F. 1998. Aquaporin-2 and -3: representatives of two subgroups of the aquaporin family colocalized in the kidney collecting duct. *Annu. Rev. Physiol.* **60:**199–220

Tanaka, S., Nomizu, M., Kurosumi, K. 1991. Intracellular sites of proteolytic processing of pro-opiomelanocortin in melanotrophs and corticotrophs in the rat pituitary. *J. Histochem. Cytochem.* **39:**809–821

Tanaka, S., Yora, T., Nakayama, K., Inoue, K., Kurosumi, K. 1997. Proteolytic processing of pro-opiomelanocortin occurs in acidifying secretory granules of AtT-20 cells. *J. Histochem. Cytochem.* **45:**425–436

Yamamoto, T., Sasaki, S. 1998. Aquaporins in the kidney: emerging new aspects. *Kidney Int.* **54:**1041–1051

Yorio, T., Bentley, P.J. 1977. Asymmetrical permeability of the integument of tree frogs (*Hylidae*). *J. Exp. Biol.* **67:**197–204

Zhang, R.B., Logee, K.A., Verkman, A.S. 1990. Expression of mRNA coding for kidney and red cell water channels in *Xenopus* oocytes. *J. Biol. Chem.* **265:**15375–15378